Citation: Molecular Therapy — Oncolytics (2016) **3,** 16004; doi:10.1038/mto.2016.4
Official journal of the American Society of Gene & Cell Therapy

www.nature.com/mto

ARTICLE

Preclinical evaluation of VAX-IP, a novel bacterial minicell-based biopharmaceutical for nonmuscle invasive bladder cancer

Shingo Tsuji[1], Xuguang Chen[2], Bryan Hancock[1], Veronica Hernandez[1], Barbara Visentin[1], Katherine Reil[1], Roger Sabbadini[1], Matthew Giacalone[1] and WT Godbey[2]

The development of new therapies that can prevent recurrence and progression of nonmuscle invasive bladder cancer remains an unmet clinical need. The continued cost of monitoring and treatment of recurrent disease, along with its high prevalence and incidence rate, is a strain on healthcare economics worldwide. The current work describes the characterization and pharmacological evaluation of VAX-IP as a novel bacterial minicell-based biopharmaceutical agent undergoing development for the treatment of nonmuscle invasive bladder cancer and other oncology indications. VAX-IP minicells selectively target two oncology-associated integrin heterodimer subtypes to deliver a unique bacterial cytolysin protein toxin, perfringolysin O, specifically to cancer cells, rapidly killing integrin-expressing murine and human urothelial cell carcinoma cells with a unique tumorlytic mechanism. The *in vivo* pharmacological evaluation of VAX-IP minicells as a single agent administered intravesically in two clinically relevant variations of a syngeneic orthotopic model of superficial bladder cancer results in a significant survival advantage with 28.6% ($P = 0.001$) and 16.7% ($P = 0.003$) of animals surviving after early or late treatment initiation, respectively. The results of these preclinical studies warrant further nonclinical and eventual clinical investigation in underserved nonmuscle invasive bladder cancer patient populations where complete cures are achievable.

Molecular Therapy — Oncolytics (2016) **3**, 16004; doi:10.1038/mto.2016.4; published online 16 March 2016

INTRODUCTION

Bladder cancer is the second most common urothelial carcinoma worldwide, the sixth leading cause of cancer death, and the fourth most common malignancy of men in developed countries.[1] An estimated 70% of bladder cancer patients present with nonmuscle invasive disease (NMIBC), with tumors confined to the mucosal surface of the uroepithelium (Ta), tumors invading the *lamina propria* but not yet the underlying muscle (T1) and carcinoma *in situ* (CIS), which can occur concomitant with TaT1 disease.[2] Currently, NMIBC patients are stratified into low-, intermediate- and high-risk disease based on tumor stage and grade in addition to other prognostic factors.[3] Treatment begins with transurethral resection of bladder tumor (TURBT) followed by risk level-appropriate post-TURBT adjuvant therapy. In intermediate and high-risk NMIBC, including those patients suffering from localized CIS, intravesical immunotherapy with the live bacterial tuberculosis vaccine Bacillus Calmette-Guerin (BCG) is the most effective adjuvant therapy treatment option. While initial responses to BCG have led to its establishment as the standard-of-care, an estimated 50% will recur and face cystectomy.[4,5] Adverse side effects with BCG range from local toxicity (occurs in 90% of patients) to more rare (<5%) but more serious systemic exposure, which can lead to sepsis, organ failure and death.[6–9] Taken together, there remains great need for less toxic alternatives to BCG as well as for bladder-sparing second line salvage therapies for use in high-risk NMIBC patients.

Bacterial minicells may provide an intriguing therapeutic option for the intravesical treatment of NMIBC as they represent an emerging class of targeted molecular delivery vehicles for therapeutic use in oncology with promising applications for tumor-specific targeted delivery of antineoplastic agents including small molecule drugs, nucleic acids and protein-based payloads.[10–12] Minicells are spherical, nano-sized particles best described as miniature versions of the bacterial cells from which they are produced, complete with all parental bacterial components except the bacterial chromosome.[13] Lacking a chromosome, minicells are inherently incapable of division, replication and persistence, and by definition, are noninfectious. Nonetheless, minicells are as amenable to recombinant engineering as proto-typical bacteria and easily designed to encapsulate specific macromolecular and small molecule therapeutic agents.

This work describes the characterization and the *in vitro* and *in vivo* evaluation of VAX-IP minicells as a recombinant bacterial minicell-based therapeutic for the intravesical treatment of NMIBC.

The first two authors contributed equally to this work.

[1]Vaxiion Therapeutics, San Diego, California, USA; [2]Department of Chemical & Biomolecular Engineering, Tulane University, New Orleans, Louisiana, USA.
Correspondence: MJ Giacalone (mjgiacalone@vaxiion.com)
Received 14 August 2015; accepted 8 January 2016

VAX-IP minicells are designed to selectively target and deliver the cholesterol-dependent membrane pore-forming protein toxin, perfringolysin O (PFO) to cancer cells expressing unligated α5 β1 (α5β1) or α3 β1 (α3β1) integrin heterodimers and results presented here demonstrate rapid, selective tumoricidal effects across a representative panel of human and murine urothelial cell carcinoma (UCC) cell lines *in vitro*.[14,15] Other *in vitro* work characterizes novel target cell plasma membrane permeabilization effects elicited by the PFO component of VAX-IP minicells, occurring in parallel with the initiation of apoptosis. The ability of VAX-IP minicells to prevent tumor growth and prolong survival after intravesical administration *in vivo* was evaluated using two clinically relevant variations of the syngeneic orthotopic murine MB49 bladder cancer model.[16] In both variations of the MB49 model, VAX-IP minicells were demonstrated to have significant dose-dependent effects on the respective growth of newly-established or well-established tumors while conferring a survival advantage with complete tumor regressions observed at the optimal therapeutic regimen. These results, along with a favorable toxicity profile, suggest the potential clinical application of VAX-IP minicells in a variety of NMIBC patient populations in addition to potential expansion into other oncology indications.

RESULTS

Strain construction, minicell generation, *in vivo* safety feature assessments, and final characterization

All minicell-producing strains and plasmids used in this study are listed in Table 1. The same genetic strategy previously described to generate the IPTG-inducible minicell-producing strain VAX8I3 was used to create a second-generation strain, coined VAX12B4, which contains *lpxM* and *dapA* gene deletions as additional safety features introduced using a combination of targeted chromosomal gene deletion techniques employing the Red recombinase system.[17,18] After confirming that both genes had been properly deleted and the minicell-producing and suicide genes had been properly integrated into the bacterial chromosome, the ability of the resulting VAX12B4 strain to produce minicells was demonstrated as shown in Figure 1a. The minicell-producing strains, VAX13E8 (*inv*+, *pfo*-), VAX15D2 (*inv*-, *pfo*+), and VAX14G8 (*inv*+, *pfo*+), were generated by the respective introduction of the tightly controlled L-rhamnose inducible recombinant expression plasmids, pVX-129, pVX-173 and pVX-156 into the background inducible minicell-producing strain VAX12B4 and used to generate VAX-I, VAX-P, and VAX-IP minicells, respectively. All minicells were generated and purified as described in the Materials and Methods section and the number of viable contaminating minicell-producing parental cells in the final minicell preparations determined by serially diluting a known number of minicells, spot plating onto MSB agar containing diaminopimelic acid (DAP) with lysine, incubating plates overnight at the permissive temperature of 30 °C and counting colony-forming units (CFU) the following day (Figure 1b). Importantly, deletion of the *dapA* gene renders minicell-producing parental cells auxotrophic for the essential bacterial cell wall intermediate, DAP. This compound is not found in high quantities in the environment nor synthesized by mammals and therefore unavailable to be scavenged *in vivo*, creating a stringent genetic safeguard against uncontrolled growth of any minicell-producing parental cells that might survive the purification process.[19] Colony counts revealed the presence of 1 viable CFU per 1.5×10^6 minicells when grown at the permissive temperature in the presence of DAP. As expected, no viable CFUs were detected when purified minicells were spot plated on to media lacking DAP and/or grown at 37 °C (Figure 1b). Furthermore, the spot plates used contained no antibiotic so that the potential presence of any adventitious microbes could be assessed prior to inclusion of material into any *in vitro* or *in vivo* studies. No visible adventitious CFUs or production cell CFUs formed within the 5-day observation period (only the 24 hours time point is shown in Figure 1b).

Bacterial lipopolysaccharide (LPS), an outer membrane component of bacteria commonly referred to as endotoxin, is known to be a potent stimulator of proinflammatory cytokine production in humans. Whether introduced through parenteral injection or a result of natural bacterial infection, systemic exposure to high levels of LPS can lead to cytokine storm, sepsis and in some cases, death. Extensive research has shown that the Lipid A component of the LPS molecule is the primary immune effector with respect to the production of proinflammatory cytokines through its interaction with mammalian cell surface-localized Toll-like receptors 2 and 4 (TLR-2 and TLR-4).[20,21] In an attempt to lessen the effects of VAX-IP minicells on the production of proinflammatory cytokines in preclinical models and eventual investigational use in humans, the *lpxM* gene of the minicell-producing strain VAX8I3 was inactivated by targeted chromosomal deletion to generate the minicell-producing strain, VAX12B4 (ref. [22]). All other minicell-producing strains used in this report were derived from VAX12B4 and each independently confirmed to be *lpxM*- by PCR analysis (not shown). Deletion of the *lpxM* gene results in the production of a modified and detoxified Lipid A component of LPS endotoxin, exhibiting marked reduction in its ability to stimulate the production of proinflammatory cytokines.[22] As shown in Figure 1c, minicells purified from VAX8I3 (*lpxM*+) generate higher peak levels of the proinflammatory cytokines TNF-α (531 ± 66 versus 171 ± 47 pg/ml, $P = 0.009$) and IL-6 (507 ± 23 versus 298 ± 33 pg/ml, $P = 0.015$) compared to those minicells purified from VAX12B4 (*lpxM*-) when incubated with primary human

Table 1 List of minicell types, bacterial strains, genotypes, and plasmids

Minicell type	*Strain*	*Genotype*	*Plasmid*
lpxM+	VAX8I3	MG1655 (*Δlac-pro, attBλ::proBA*ΩpTac::*ftsZ*Ω*c1857*-PR-PL::*I-CeuI*)	None
Vector (*lpxM*-)	VAX12B4	MG1655 (*Δlac-pro, ΔlpxM, ΔdapA, attBλ::proBA*ΩpTac::*ftsZ*Ω*c1857*-PR-PL::*I-CeuI*)	None
VAX-I	VAX13G8	isogenic to VAX12B4	pVX-129 (*inv*+, *pfo*-)
VAX-P	VAX15D2	isogenic to VAX12B4	pVX-173 (*inv*-, *pfo*+)
VAX-IP	VAX14G8	isogenic to VAX12B4	pVX-156 (*inv*+, *pfo*+)

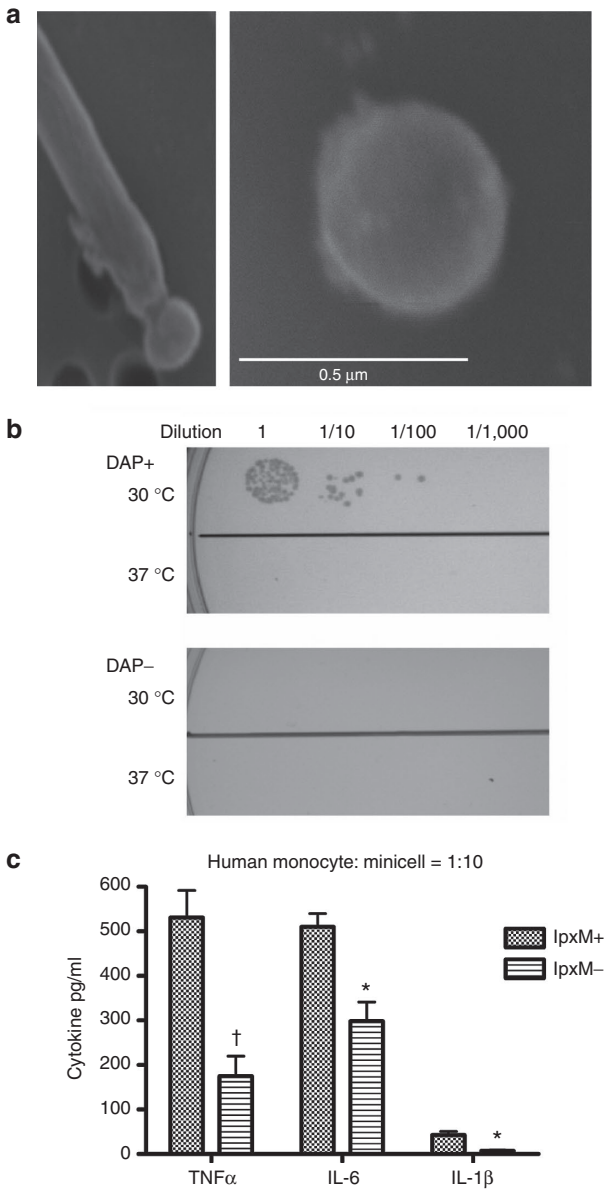

Figure 1 Characterization of representative bacterial minicell-producing strain VAX14G8. (**a**) The inducible VAX-IP minicell producing *E. coli* strain VAX14G8 shown actively producing a minicell from the polar region of a rod-shaped parental cell after addition of IPTG (left panel) and an isolated minicell (right panel). (**b**) Temperature-induced suicide phenotype of the VAX-IP minicell producing strain VAX14G8 (upper panel) and dependence on the presence of diaminopimelic acid (DAP) for parental cell growth (lower panel). (**c**) Inflammatory cytokine production from primary human monocytes after a 6-hour exposure to either wild-type (*lpxM*+) or lipopolysaccharide-mutant (*lpxM*-) minicells at a fixed ratio of minicells to monocytes of 10. * denotes $P \leq 0.05$; † denotes $P \leq 0.01$.

monocytes at a ratio of minicells to monocytes of 10:1. A lesser yet still significant decrease in Interleukin-1β (IL-1β) was also observed (44 ± 6 versus 6 ± 3 pg/ml, $P = 0.014$).

After purification of minicells, determination of the number of parental contaminants, and ensuring DAP dependence in parallel with the activity of the temperature sensitive genetic suicide mechanism of residual parental cells, minicells were analyzed for their expression and minicell-surface localization of Invasin by western blot and flow cytometry, respectively (Figure 2a,b). As shown in Figure 2a, Invasin is readily detectable by western blot in VAX-IP minicells but not in VAX-P minicells (*inv*-) as demonstrated by the blots conducted on whole VAX-IP minicell lysates compared to the signal detected for the positive control, a purified recombinant protein fusing Invasin to the maltose binding protein (MBP-Inv).[23] Figure 2b demonstrates that the overall percentage of VAX-IP and VAX-I minicells displaying Invasin on their surfaces was nearly equivalent at 91 ± 3.5% versus 93 ± 1.7% as was determined by the detection of mAb3A2 by goat anti-mouse Alexa Flour 488-conjugated secondary antibody using flow cytometry. No appreciable signal was detected in the controls for these experiments which included the parallel analysis of an equivalent number of VAX-P minicells (*inv* -), an isotype matched mouse nonspecific primary antibody control (coincubated with VAX-I minicells) and a secondary reagent-only control.

Following characterization of the expression and proper surface location of the Invasin component, different minicell types were then evaluated for their respective perfringolysin O (PFO) contents and hemolytic activity levels (Figure 2c,d), the latter of which is commonly utilized to measure the functional activity of PFO.[15] The western blot presented in Figure 2c demonstrates the presence of PFO in VAX-P and VAX-IP minicells compared to a standard curve generated from varying concentrations of purified recombinant PFO (rPFO). The corresponding hemolytic activity of PFO in VAX-IP minicell lysates shown in Figure 2d was used to determine the amount of active PFO present per intact (nonlysed) minicell equivalent as compared to that of the VAX-I (*pfo* -) minicell lysates and a corresponding rPFO control. Hemolytic activity equal to that of VAX-IP lysates was observed for VAX-P lysates (not shown). Using data obtained from these two experiments, it was determined that approximately 45 ng of PFO was present in 1×10^8 VAX-IP or VAX-P minicells. Having demonstrated that VAX-IP minicells carry an active payload, PFO, and that the integrin-targeting moiety, Invasin, is expressed on the minicell surface, the roles of these components in killing cancer cells *in vitro* was then evaluated.

Integrin expression and Invasin-mediated internalization of minicells into bladder cancer cell lines *in vitro*

Prior to performing cell-killing experiments, the ability of minicells expressing Invasin to be internalized by a panel of murine and human bladder cancer cells was assessed using a combination of fluorescent microscopy and flow cytometry techniques. These experiments made use of VAX-I minicells as it was found that VAX-IP minicells killed cells quite rapidly (see below) and as a result, measuring uptake kinetics in live cells would prove difficult in the presence of PFO. As shown in Figure 3, Invasin-expressing VAX-I minicells are rapidly internalized into each of MB49, RT4, and T24 bladder cancer cells compared to those "native" vector *E. coli* minicells (*inv-, pfo*-) as was determined by immunocytochemistry using a minicell-specific rabbit polyclonal antibody as the primary detection reagent. To differentiate between those minicells that were truly internalized versus those that were merely bound to the cancer cell surface, fixed and permeabilized cells were compared to those cells that had been only fixed, respectively. As is demonstrated in the fluorescence microscopy images of Figure 3, minicell uptake and localization to the cell interior is Invasin-dependent. In contrast, minicells lacking Invasin were not significantly internalized by any cell type tested within the 2-hour treatment window. These results were confirmed by flow cytometry where an increase in relative fluorescence is observed in those VAX-I-treated cells that had been both fixed and permeabilized. Interestingly, when minicells

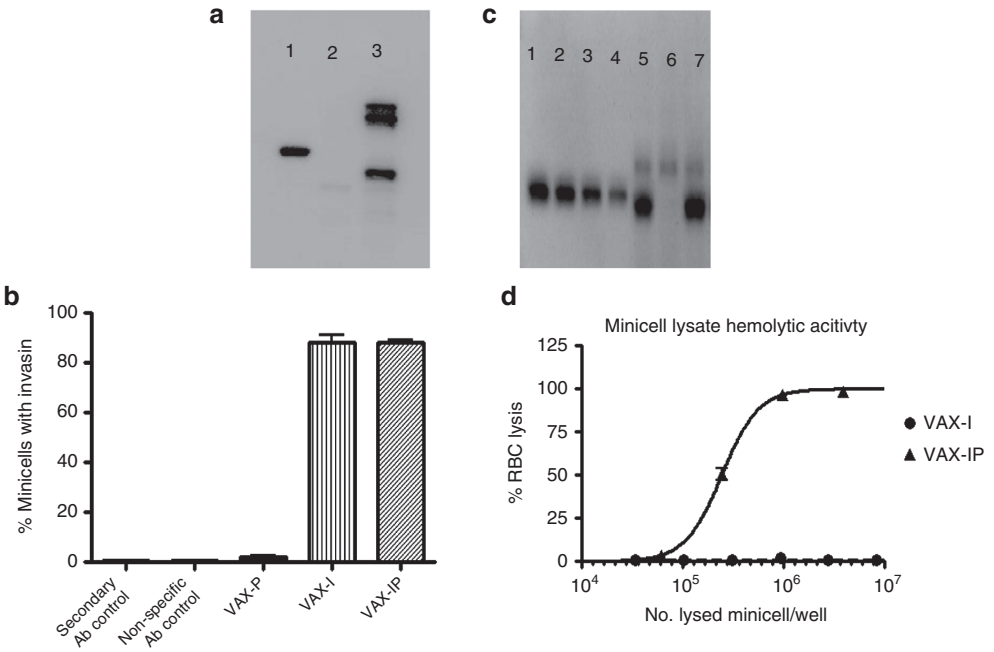

Figure 2 Characterization of VAX-IP minicells. (**a**) The Invasin content of VAX-IP minicells (lane 3) was determined by western blot using the anti-Invasin monoclonal antibody mAb3A2 as compared to 500 ng of purified maltose-binding protein-Invasin fusion protein standard (lane 1) or an equivalent number of VAX-P minicells (no Invasin gene, lane 2). (**b**) The surface localization of Invasin in VAX-I (no perfringolysin O (PFO)) and VAX-IP minicells was determined by flow cytometry using mAb3A2 as the primary detection antibody. VAX-P minicells were analyzed as a negative control. (**c**) The PFO content of VAX-IP minicells (lane 7) was determined by western blot using the anti-PFO monoclonal antibody mAb3H10 against a titrated recombinant PFO (rPFO) standard (lanes 1–4), VAX-P minicells (lane 5), and VAX-I minicells (lane 6). (**d**) The PFO-mediated hemolytic activity against sheep red blood cells was determined using diluted lysates of VAX-IP or VAX-I (no PFO) minicells.

lacking Invasin were incubated with bladder cancer cell lines for longer than 6 hours, some degree of internalization is achieved in each cell type (not shown). It may be that the presence of FimH on the surface of *E. coli* minicells is promoting generalized uptake through sustained interaction with cell surface mannose residues and the mannose binding lectin domain of FimH or with uroplakin Ia as has also been reported.[24,25]

Cytotoxicity of VAX-IP minicells across a panel of human and murine bladder cancer cell lines *in vitro*

The cytotoxicity of VAX-IP minicells compared to VAX-I minicells or to an amount of purified recombinant PFO (rPFO) equivalent to the amount of PFO delivered by VAX-IP minicells was evaluated *in vitro* across a panel of human and murine bladder cancer cell lines. Potency of VAX-IP minicells, as measured by cytotoxicity *in vitro*, was demonstrated using a standard dose–response curve quantified by using the ratio of the number of minicells added per plated mammalian cell, denoted as the "multiplicity of infection" (MOI) needed to achieve 50% growth inhibition (IC_{50}). As demonstrated in Figure 4a, VAX-IP minicells had a profound cell killing effect following a 24-hour exposure across all urothelial cell carcinoma cell lines tested, whereas an equivalent number of VAX-I minicells had no effect. No killing was observed with rPFO at those concentrations used in MB49 and RT4 cell lines. In the case of T24 and HTB-9 (both high-grade human urothelial carcinomas), killing with rPFO was observed, but the respective IC_{50} values of rPFO ranged from 10- to 2,500-fold the amount of PFO found to be effective when the payload is delivered intracellularly by VAX-IP minicells, underscoring the value of the minicell carrier as an effective-targeted drug delivery vehicle.

Because the typical exposure time to intravesically administered therapeutic agents for the treatment of NMIBC in the clinical setting is usually limited to a maximum of 2 hours, the ability of VAX-IP minicells to exert their cytotoxic effects *in vitro* within this timeframe was examined. As also shown in Figure 4a, VAX-IP minicells were nearly as cytotoxic following a 2-hour exposure in comparison to a 24-hour exposure in all urothelial cell carcinoma cell lines tested, providing confidence that this agent has the potential to be effective in a more clinically-relevant timeframe where exposure time is limited. After determining the potency, kinetics, and broad-spectrum activity of VAX-IP minicells across this select panel of representative human and murine UCC cell lines, attention was then turned to elucidating the mechanism of cytotoxicity.

Mechanism of cytotoxicity of VAX-IP minicells *in vitro*

Given that PFO is a cholesterol-dependent membrane pore-forming protein, it stands to reason that the primary mechanism of action of PFO is lysis of the tumor cell plasma membrane or other subcellular cholesterol containing membranes.[15,26,27] To elucidate this potential mechanism, the presence of lactate dehydrogenase (LDH) enzymatic activity in the cell culture media of VAX-IP minicell-treated cells was evaluated. As it is normally found in the cytosol of mammalian cells, the enzymatic activity of LDH in the media of cultured cells is a commonly used methodology to determine plasma membrane integrity.[28] As shown in Figure 4b, low levels of LDH activity were observed as soon as 20 minutes after MB49 cells were treated with VAX-IP minicells and full LDH activity signal was achieved by 90 minutes. In contrast, no LDH activity was detected when an equivalent amount of PFO deficient VAX-I minicells (*pfo* -) was added. Importantly, rPFO was unable to kill cultured cells at a concentration of PFO equivalent to that contained within VAX-IP minicells, demonstrating the critical utility of intact minicells to kill cells through intracellular

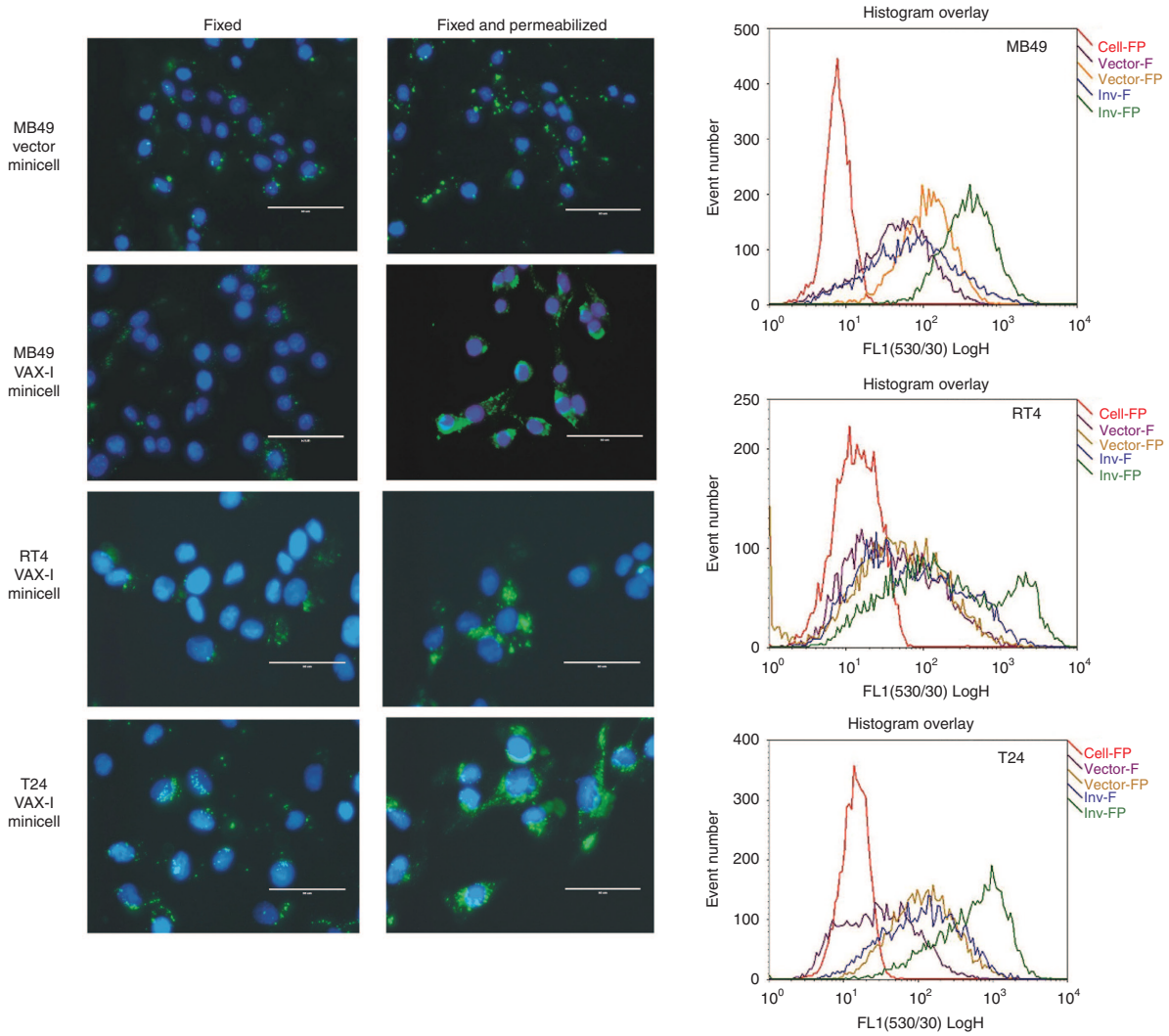

Figure 3 Invasin-mediated uptake into bladder cancer cells. Purified native "vector" minicells (top panels) and VAX-I minicells (lower three panels), were incubated with murine urothelial cell carcinoma cell line MB49, low-grade human papillary urothelial carcinoma cell line RT4, or high-grade human urothelial carcinoma cell line T24. After a 2-hour incubation, cells were washed and fixed (left panels) or fixed and permeabilized (center panels) and minicell localization determined by immunohistocytochemistry using a polyclonal antibody against minicells as the primary detection antibody. Cells were also analyzed for mean fluorescence by flow cytometry (right panels).

delivery of encapsulated PFO toxin (Figure 4a). Interestingly, rPFO added to the cell culture media caused maximal LDH release into cell culture supernatants with much faster kinetics than VAX-IP minicells (Figure 4b). The delay in LDH release observed with VAX-IP minicell-treated cells versus that of rPFO-treated cells probably reflects the time needed for VAX-IP minicells to be internalized into endosomes and undergo degradation to release enough PFO toxin payload to see its membrane permeabilizing effect. Despite much faster LDH release kinetics and enzymatic activity levels, rPFO was not able to kill cells, even at the 24-hour time point (see Figure 4a), suggesting that a transient permeabilization of the plasma membrane using the concentrations of rPFO used in these experiments is not sufficient to kill cells. Cell killing requires encapsulation and intracellular delivery of PFO to target cells.

To confirm that the target cell plasma membrane integrity was compromised following exposure to VAX-IP minicells and that LDH release was not being detected by some alternative phenomena, VAX-IP minicell-treated cells were analyzed for their abilities to allow entry of propidium iodide (PI). Propidium iodide is a nonmembrane permeable fluorescent nucleic acid binding compound commonly used to confirm membrane integrity. Cells with intact plasma membranes exclude entry of propidium iodide, whereas cells with permeabilized plasma membranes allow rapid entry into cells, interaction with intracellular nucleic acids and a resulting nucleic acid intercalation-dependent increase in fluorescence.[29] As shown in Figure 4c, MB49 cells exposed to VAX-IP minicells for 2 hours were positive for PI staining as determined by flow cytometry. In comparison, those MB49 cells left untreated or that were treated with an equivalent amount of VAX-I minicells were largely able to exclude PI and as a consequence stained negatively. The release of LDH into cell culture supernatant taken in combination with these PI data strongly support the hypothesis that PFO-mediated permeabilization and destabilization of the target cell plasma membrane is a mechanism of action contributing to the observed cytotoxicity of VAX-IP minicells *in vitro*. However, as evidenced by the unexpected finding that exogenously added rPFO results in full

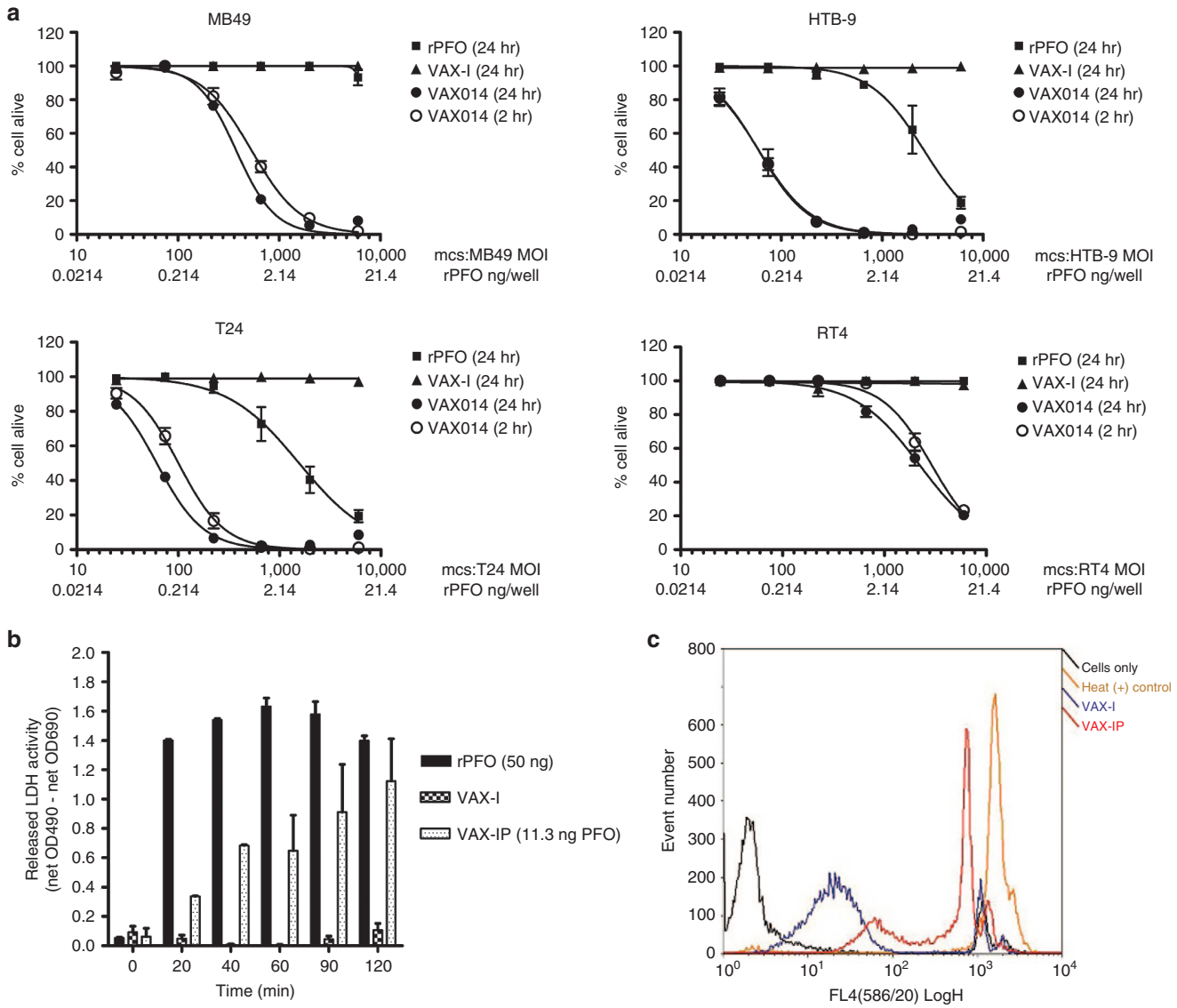

Figure 4 Rapid perfringolysin O (PFO)-dependent cytotoxicity of VAX-IP in relevant bladder cancer cell lines. (**a**) The number of VAX-IP or VAX-I minicells needed to kill murine MB49, human RT4, human HTB-9, and human T24 urothelial cell carcinoma cell lines, expressed as the ratio of minicells to plated mammalian cell, was assessed by addition of PrestoBlue viability dye after a 24-hour coincubation. (**b**) PFO-dependent plasma membrane permeabilization and release of lactate dehydrogenase (LDH) into cell culture supernatants was assessed in MB49 cells over a 2-hour time course as compared to recombinant PFO (rPFO) and an equivalent number of VAX-I minicells. (**c**) PFO-dependent plasma membrane permeabilization was also assessed by propidium iodide staining of MB49 cells treated with VAX-IP for 2 hours as compared to an equivalent number of VAX-I minicells and compared to negative (cells only) and positive (heat treated) controls.

LDH release and membrane permeabilization but not necessarily in cell death, the possible role of apoptosis was explored (Figure 5a–c).

Evidence of apoptosis in response to VAX-IP minicells *in vitro*

Evidence of VAX-IP minicell-mediated apoptosis in cultured cells was analyzed using three different methods including an assessment of condensed/pyknotic nuclei, loss of mitochondria membrane potential, and activation of key caspases in response to VAX-IP minicell treatment *in vitro*. One of the classic hallmarks of apoptosis is condensation of nuclei, nuclear fragmentation and appearance of punctuate nuclear structures or pyknotic nuclei. As shown in Figure 5a, MB49 cells exposed to VAX-IP minicells for 24 hours appear smaller and more granular as demonstrated after examination by light microscopy (lower left panel) compared to untreated cells (upper left panel). In addition, staining of nuclear DNA with DAPI reveals nuclear condensation and the presence of pyknotic nuclei under examination by fluorescence microscopy (lower right panel) as compared to DAPI-stained untreated control cells (upper right panel).

Another hallmark of apoptosis is the destabilization of mitochondria, resulting in a collapse of mitochondrial membrane potential ($\Delta\psi m$) and mitochondrial membrane permeabilization (MMP), ultimately resulting in the release of additional proapoptotic mitochondrial factors such as cytochrome C, HSP60 and apoptosis-inducing factor (AIF) into the cytosol.[30,31] Mitochondrial membrane potential is commonly assayed by flow cytometry in conjunction with the use of the mitochondrial membrane specific fluorescent dye, MitoTracker RedCMXRos (Molecular Probes, Eugene, OR). As demonstrated in Figure 5b, MB49 cells stained with MitoTracker RedCMXRos exhibit a marked loss in fluorescence intensity when

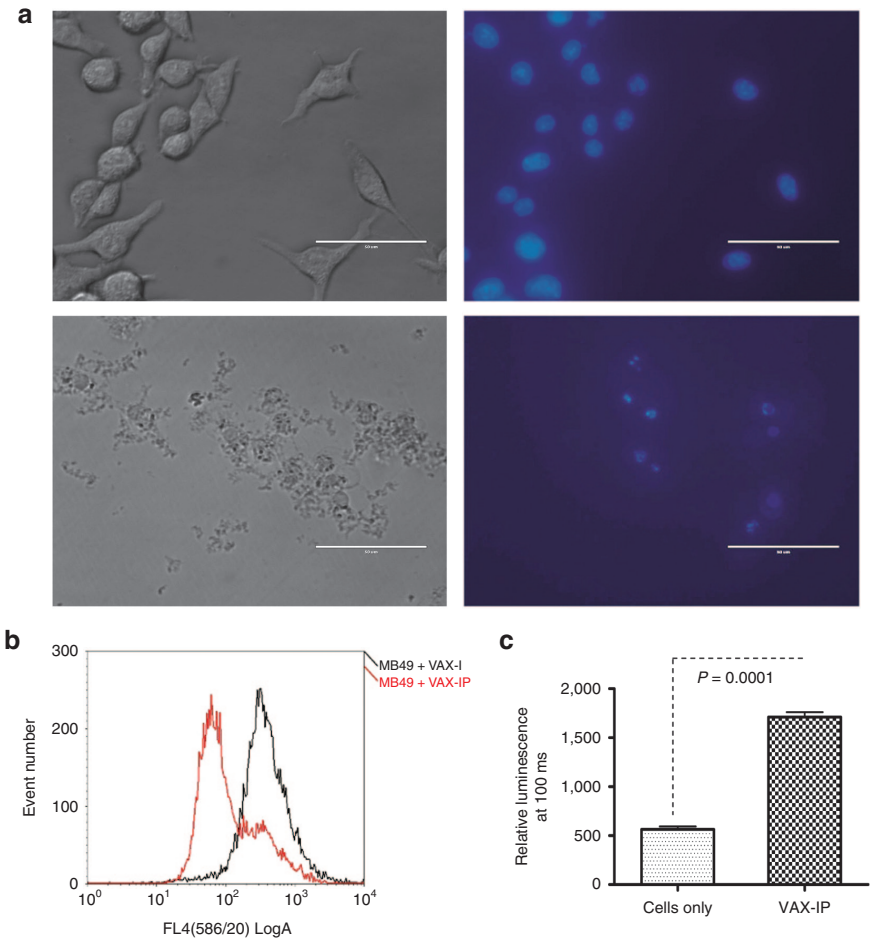

Figure 5 Hallmarks of apoptosis in cells following treatment with VAX-IP. (**a**) The development of pyknotic and condensed nuclei in response to VAX-IP was evaluated in cultured MB49 cells after a 2-hour exposure at a ratio of VAX-IP minicells to plated MB49 cells of 5,000:1. Following treatment, cells were stained for 5 minutes with DAPI and visualized by fluorescence microscopy at 40×. (**b**) Loss of mitochondrial potential in response to treatment with VAX-IP was determined by flow cytometry on cells stained with MitoTracker RedCMXRos after a 2-hour exposure to VAX-IP at a ratio of VAX-IP minicells to plated MB49 cells of 5,000:1. (**c**) Activation of Caspase 3/7 was assessed after cells were subjected to a 3-hour exposure to VAX-IP followed by overnight incubation after which caspase activity was measured using the Caspase-Glo 3/7 assay.

exposed to VAX-IP minicells as opposed to those cells treated with an equivalent amount of VAX-I (*pfo* -) minicells. This finding indicates a PFO-dependent, VAX-IP minicell-mediated loss in $\Delta\psi m$ and suggests apoptosis plays a role in the cytotoxic response to VAX-IP minicells *in vitro*.

In confirming the role of apoptosis as suggested by Figure 5b, Figure 5c demonstrates that MB49 cells exhibit a threefold increase ($P = 0.0001$, $n = 3$ independent experiments) in the activity of effector caspases 3 and/or 7 as measured by an increase in caspase enzymatic activity using the Caspase-Glo 3/7 assay (Promega Corporation, Madison, WI) following a 3-hour exposure to VAX-IP minicells compared to untreated controls. While more work will be required to delineate more precisely the definitive apoptogenic pathway(s) contributing to VAX-IP minicell cytotoxicity *in vitro*, the work presented here clearly demonstrate a role for apoptosis.

Integrin-dependent cytotoxicity of VAX-IP minicells

Several different experiments were conducted to confirm that VAX-IP minicells mediate their rapid *in vitro* cell killing effect through the interaction of the Invasin component with α3 β1 (α3β1) and α5 β1 (α5β1) integrins heterodimers (Figure 6a–f). This was presumed to be the case at the outset of this work as Invasin has been demonstrated to work equally well to stimulate internalization into either human or murine cells through its interaction with α5β1 or α3β1 (refs. [32,33]). Prior to performing cytotoxicity experiments against cultured bladder cancer cell lines with VAX-IP minicells *in vitro*, the integrin expression profiles of both RT4 human papillary urothelial cell bladder carcinoma and the murine MB49 bladder cancer cell lines planned for the syngeneic orthotopic model were determined. As shown in Figure 6c,f, MB49 had strong levels of β1 expression and α5 subunit expression, whereas RT4 had strong levels of β1 expression with low α5 subunit expression and high α3 subunit expression. The expression of murine α3 subunit was not analyzed as there is no commercially available function blocking antibody specific for the murine α3 integrin subunit. The expression of β1, α3, and α5 integrins was also confirmed in human T24 and HTB-9 bladder cancer cell lines where high levels of α5 and α3 integrins were respectively observed (not shown).

To determine whether the interaction of the Invasin component of VAX-IP minicells with either α3β1 or α5β1 integrins was required to achieve targeted tumor cell killing, the ability of VAX-IP minicells to kill integrin expressing murine MB49 or human RT4 bladder cancer cell lines in the presence of integrin-specific or Invasin-specific function blocking antibodies was evaluated *in vitro*.[23,34,35] Invasin and fibronectin bind a mutually exclusive overlapping site within the α5β1 integrin.[36] Therefore, the integrin-specific function-blocking

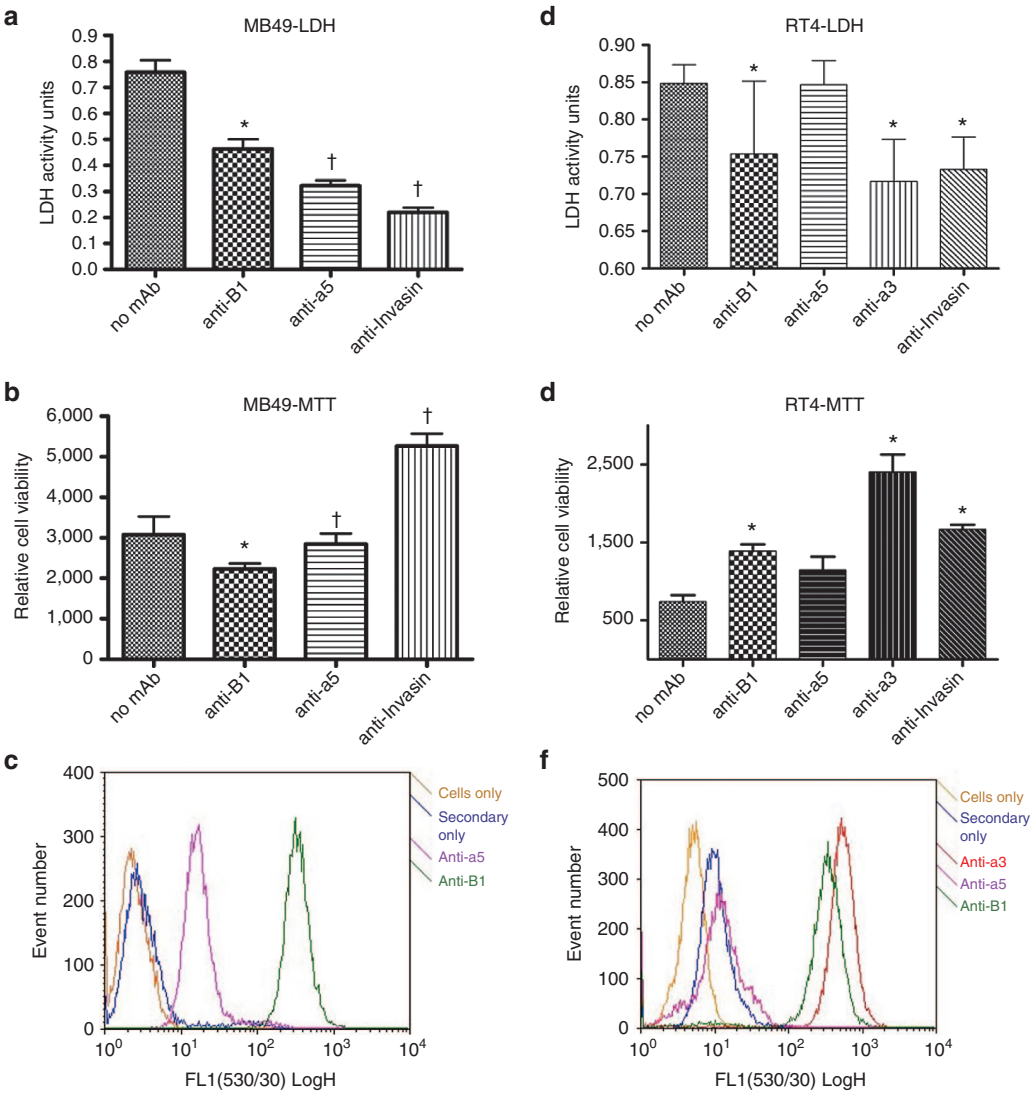

Figure 6 Integrin-specificity of VAX-IP. (**a–c**) The ability of VAX-IP to stimulate LDH release (**a**) and cell killing (**b**) in MB49 cells was assessed in the presence of function blocking anti-mouse β1 or α5 integrin antibodies as well as with VAX-IP minicells preincubated with the Invasin function blocking monoclonal antibody mAb3A2. The relative expression levels of both β1 and α5 in MB49 is demonstrated by flow cytometry using the same function blocking antibodies as primary detection reagents (**c**). (**d–f**) The ability of VAX-IP to stimulate LDH release (**d**) and cell killing (**e**) in RT4 cells was assessed in the presence of function blocking anti-human β1, α3, or α5 integrin antibodies as well as with VAX-IP minicells preincubated with the Invasin function blocking monoclonal antibody mAb3A2 or an irrelevant antibody control. The relative expression levels of β1, α3, and α5 in RT4 is demonstrated by flow cytometry using the same function blocking antibodies as primary detection reagents (**f**). * denotes $P \leq 0.05$; † denotes $P \leq 0.005$.

antibodies used for these studies were carefully selected for their ability to prevent integrin-mediated binding to fibronectin or laminin, for α5 and α3 integrins, knowing that these antibodies would likely also inhibit binding to Invasin through the same mutually exclusive binding site. Prior to performing these experiments, a second confirmation of integrin expression via flow cytometry was conducted to ensure that integrin expression had not changed during routine cell cultivation. The presence of function-blocking integrin-specific antibodies resulted in concomitant reduction in VAX-IP minicell-mediated cell killing (Figure 6b) and LDH release (Figure 6a) in MB49 cells with a 1.7-fold increase in cell viability and a 37% reduction in LDH release for β1 blocking antibodies ($P = 0.01$) or a 2-fold increase in cell viability and a 53% reduction in LDH release for α5 blocking antibodies ($P = 0.002$). Preincubation of VAX-IP minicells with the Invasin-specific blocking antibody, mAb3A2, prior to addition to tumor cells also resulted in a 2.3-fold reduction in cell killing and a 70.6% reduction in LDH release ($P = 0.001$). Similar results were obtained in experiments conducted in human RT4 bladder cancer cells using integrin-specific blocking antibodies against either α3 subunit (3.2-fold reduction in cell killing and 18% reduction in LDH release, $P = 0.03$), or β1 integrin subunit (1.6-fold reduction in cell killing and 15% reduction in LDH release, $P = 0.05$) as is shown in Figure 6d,e. The introduction of function-blocking α5 integrin subunit antibodies had only a slight effect on cell killing (1.4-fold reduction) and lead to no reduction in LDH release. Figure 6f demonstrates that RT4 expresses α3 integrin at high levels and α5 integrin at very low levels, drawing a strong correlation to the results in Figure 6d,e where the largest reductions in cell killing and LDH release were seen with the anti-α3 function-blocking antibodies versus that of the anti-α5 function-blocking antibodies. Taken together, these studies confirm the findings of previous reports on the integrin specificity of Invasin by demonstrating that blockade of the Invasin binding site of α5 integrin or α3 integrin with function-blocking antibodies can inhibit Invasin-mediated internalization

and cell-killing properties of VAX-IP minicells. Additionally, these results combine to illustrate that Invasin works to promote integrin-mediated internalization and VAX-IP minicell-mediated killing of both human and murine cell lines. Because integrins are so highly conserved in structure, function and spatial expression amongst mammalian species, the species-agnostic integrin binding properties of Invasin and of VAX-IP minicells will help to better ensure that *in vivo* pharmacology and toxicology results obtained from evaluations made in murine models have a higher probability of translating into large animals and ultimately into humans.

Dose range finding studies conducted in the late treatment variation of established syngeneic orthotopic MB49 tumors

To establish doses for survival experiments, a preliminary dose range finding study following topical intravesical instillation of VAX-IP minicells through a urinary catheter was performed using the "late treatment" variation of the syngeneic orthotopic MB49 murine bladder cancer model. This particular variation of the orthotopic MB49 model was selected for dose range finding studies because it is aggressive and difficult to treat.[37,38] Therefore, it was considered that any reduction in tumor burden as measured by overall post mortem bladder weight using the late treatment variation of this model would likely translate well to other model variations. The late treatment variation utilized 100,000 MB49 cells and treatments were not initiated until 5 days post-tumor cell instillation (day 6), when tumors were established to the point of being digitally palpable and concomitant gross hematuria was present. As shown in Figure 7a, the median and average bladder weights, surrogates for tumor burden, decreased with increasing doses of VAX-IP minicells when given via topical intravesical instillation via urinary catheter. Doses were administered at 5×10^6, 5×10^7, 1×10^8, 5×10^8, and 1×10^9 VAX-IP minicells per mouse. A significant difference over saline-treated control animals (median bladder weight 170.3 mg, mean of 179.8 ± SD of 77.2 mg, range of 91.9–341.3 mg) was found at dose levels of 1×10^8 VAX-IP minicells (median bladder weight 52.6 mg, mean of 108.8 ± SD of 122.8 mg, range of 24.2–361.9 mg, $P = 0.006$) and again at 5×10^8 (median bladder weight 65.8 mg, mean of 60.9 ± SD of 24.9 mg, range 33.0–106.7 mg, $P = 0.0002$). Curiously, the highest dose (10^9 VAX-IP minicells) demonstrated less profound effects on tumor burden (median bladder weight 107.7 mg, mean of 244.1 ± SD of 237.8 mg, $P = 0.74$). Regardless of the dose level given, no evidence of observed bladder-localized adverse events (gross hematuria, micturition frequency, and cystitis) or evidence of systemic adverse events (fever, chills, and cachexia) were recorded, suggesting a favorable safety profile of VAX-IP minicells administered via topical intravesical instillation.

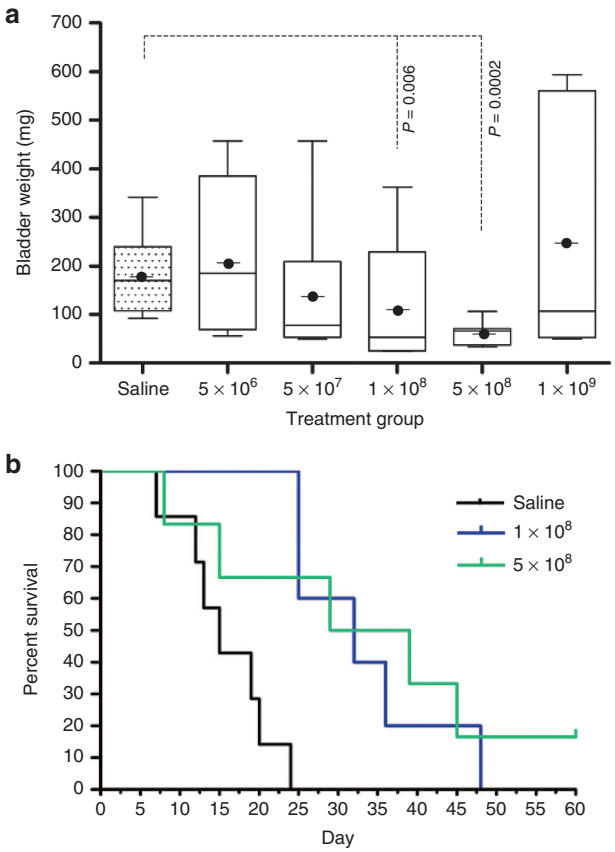

Figure 7 Efficacy of VAX-IP minicells in the late treatment of murine syngeneic orthotopic MB49 bladder tumors. Orthotopic bladder tumors were established by installation of 100,000 MB49 murine bladder cancer cells on day 0. Treatments were initiated on day 6 and given every 3 days thereafter for a total of five doses. (**a**) Preliminary dose range finding studies were conducted using a range of VAX-IP minicells. Animals were sacrificed on day 19 and bladders were removed, weighed, and recorded as a surrogate for bladder tumor burden. (**b**) Using the doses and dose regimen established in the dose range finding studies, the experiment was repeated with two dose groups, 1×10^8 ($n = 6$), and 5×10^8 ($n = 7$), and compared to saline-treated controls ($n = 9$). Animals were observed daily throughout a 60-day in-life observation period.

Effect of VAX-IP minicells on survival in the late treatment of established orthotopic MB49 tumors *in vivo*

The ability of VAX-IP minicells to prevent tumor outgrowth and prolong survival of mice bearing syngeneic orthotopic tumors was evaluated using the "late treatment" variation of the MB49 model where treatment initiation is delayed 5 days after tumor installation. From the standpoint of clinical relevance, the late treatment model most closely mimics situations where carcinoma *in situ* (CIS) is present. In these patients, surgical resection options may be limited and induction therapy is given when CIS is well established. Using the dose range information gathered in bladder weight experiments using this model variation (Figure 7a), treatment groups included vehicle only (saline control), 1×10^8 VAX-IP minicells, or 5×10^8 VAX-IP minicells. Treatments were initiated on day 6 and administered every 3 days thereafter for a total of five doses. Following a 60-day observation period, the experiment was halted, surviving animals euthanized and bladders removed to confirm the presence or absence of tumor via histological examination of sectioned bladders and compared to the bladders of animals that had succumbed to tumor burden during the study. The results shown in Figure 7b demonstrate a statistically significant survival advantage was achieved in animals treated with either dose. A dose of 1×10^8 VAX-IP minicells resulted in an overall median survival of 32 days (range of 25 to 48 days) compared to 15 days (range of 7 to 24 days) for saline-treated animals ($P = 0.001$) with no animals surviving at the end of the 60-day observation period. Similarly, a dose of 5×10^8 VAX-IP minicells resulted in an overall median survival of 34 days (range of 8 to over 60 days) compared to 15 days (range of 7 to 24 days) for saline-treated animals ($P = 0.003$) with 16.7% of animals surviving at the end of the 60-day observation period. Again, using this variation of the MB49 model, no evidence of observed bladder-localized adverse events (gross hematuria, micturition

frequency, and cystitis) or evidence of systemic adverse events (fever, chills, and cachexia) were recorded.

Effect of VAX-IP minicells on survival in the early treatment of orthotopic MB49 tumors in vivo

The ability of VAX-IP to prevent tumor outgrowth and prolong survival of mice bearing syngeneic orthotopic tumors was evaluated in a dose-escalation study with intravesical treatments applied once weekly for 4 weeks and initiated early (24 hours) after tumor implantation.[16] This "early treatment" variation of the MB49 orthotopic model is designed to mimic the clinical scenario where incomplete resection results in low-level residual tumor burden or where undetected secondary tumor(s) exist, phenomena commonly thought to be associated with tumor recurrence in NMIBC patients. Using the information gathered in the dose range finding study in combination with that used in the survival study employing the late treatment model variation, a dose of 1×10^8 VAX-IP minicells was compared to saline-treated control. Following the 60-day observation period, the experiment was halted, surviving animals euthanized and bladders removed to confirm the presence or absence of tumor via histological examination as compared to the bladders of animals that had succumbed to tumor burden during the study. The results shown in Figure 8 demonstrate that a statistically significant survival advantage was observed in animals treated with 1×10^8 VAX-IP minicells with an overall median survival of 38 days (range of 15 to over 60 days) compared to 15 days (range of 7 to 24 days) for saline-treated animals ($P = 0.001$) with 28.6% of animals surviving at the end of the 60-day observation period.

DISCUSSION

In this report, the development, characterization and pharmacological activity of VAX-IP minicells, a novel recombinant bacterial minicell-based biopharmaceutical product candidate being developed for the treatment of NMIBC is described. The results of these experiments demonstrate that VAX-IP minicells have significant, dose-dependent antitumor effects that can result in tumor regression while conferring a survival advantage over untreated animals in two clinically relevant variations of the syngeneic orthotopic murine MB49 model of superficial bladder cancer. The therapeutic benefits of VAX-IP minicells were observed in both the "early treatment" variation of the model, where it outperforms what has been reported for BCG, and the "late treatment" variation of the model, in which BCG has been reported to have no effect.[16,39] Improvement over what has been reported for BCG in the MB49 model may be a function of VAX-IP minicells' unique dual specificity for $\alpha5\beta1$ and $\alpha3\beta1$ integrins, rapid killing properties and the unique mechanism of action demonstrated by the *in vitro* work described in this report and elaborated upon below. Interestingly, the therapeutic effect *in vivo* seemed to lessen when given beyond the optimal dose range when adminstered intravesically twice weekly in the late treatment variation of the MB49 model. While the cause of this remains unknown, similar results have been reported for other clinical stage compounds evaluated preclinically using the MB49 model. Of particular interest is that BCG has been shown to lose its immunotherapeutic effect at higher doses. In both preclinical models as well as in the clinical setting the loss of effect is associated with a dose-dependent shift in immune response from Th1 to Th2 at the higher and less effective dose and this "bell-shaped" dose–response curve has been reported for other immunotherapeutics.[40,41] Given the bacterial nature of minicells, the possibility exists that VAX-IP minicells also stimulate a localized immunotherapeutic response in addition to a direct selective cytotoxic effect when administered intravesically *in vivo*. Though outside the scope of the work presented here, this is an area of intense ongoing investigation.

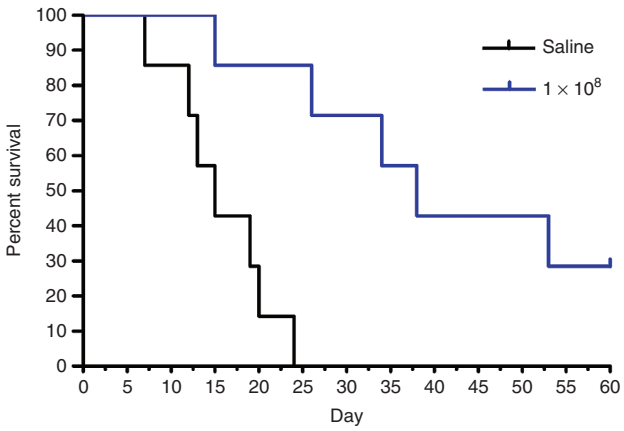

Figure 8 Efficacy of VAX-IP minicells in the early treatment of murine syngeneic orthotopic MB49 bladder tumors. Orthotopic bladder tumors were established by installation of 100,000 MB49 murine bladder cancer cells on day 0. Treatments were initiated on day 1 and given every 7 days thereafter for a total of four doses. Using the doses and dose regimen established in the dose range finding studies, the experiment was conducted with 1×10^8 ($n = 7$) VAX-IP minicells and compared to saline-treated controls ($n = 9$). Animals were observed daily throughout a 60-day in-life observation period.

Unlike BCG or other cytotoxic agents evaluated for use in NMIBC or in the MB49 model, VAX-IP minicells have a unique cytolytic mechanism of action resulting from the VAX-IP minicell-mediated intracellular delivery of PFO to tumor cells. In evidence of this, it was found that the addition of recombinant PFO (rPFO) to cultured bladder cancer cells quickly and transiently permeabilizes the plasma membrane of cells, but cells fully recover and are completely viable even after a 24-hour exposure to rPFO at concentrations equivalent to those present in VAX-IP minicells. In stark contrast, delivery of the same concentration of PFO to cells using VAX-IP minicells to drive endosomal delivery of this membrane pore-forming toxin still results in permeabilization and release of cytoplasmic contents, but also in concomitant apoptosis and rapid cell death. The apoptosis work presented here is convincing but cursory in nature and investigation into more definitive mechanisms and involvement of proapoptotic pathways is under way. One distinct possibility that could explain why the intracellular delivery of PFO cause cell death and stimulates apoptosis is that PFO is mediating release of endosomal cathepsins into the cytosol, or that PFO itself escapes the endosome and forms pores in cholesterol-containing membranes of mitochondria and other subcellular organelles. Both the release of cathepsins to the cytosol and mitochondria membrane permeabilization have been identified as initiators of apoptosis.[30,31,42] Interestingly, purified recombinant PFO has been used to transiently and selectively permeabilize cells in the research of mitochondrial membrane potential, however PFO has never been reported to have a therapeutic effect via a mitochondrial specific mechanism either *in vitro* or *in vivo*.[43] The presence of Invasin on the surface of VAX-IP minicells ensures that tumor cell internalization and killing occurs within 2 hours while conferring selectivity of VAX-IP minicells for tumor cells expressing either or both of $\alpha5\beta1$ or $\alpha3\beta1$ integrins. The rapid killing properties of VAX-IP minicells cannot be understated in the context of its intended

clinical utility as agents given intravesically for the treatment of NMIBC are only left in the bladder for direct exposure to tumor as a topical therapy for a period of 2 hours or less.

The ability of VAX-IP minicells to selectively target and rapidly kill tumor cells expressing either or both of α5β1 and α3β1 in the context of NMIBC may be of critical importance in the treatment of high-risk BCG unresponsive patients when integrin expression patterns in NMIBC are considered. In normal urothelium, α5β1 is not detectable whereas α3β1 is expressed but confined to the basal surface of the urothelium and the interstitial spaces at cellular junctions where it is thought to promote cell-to-cell adhesion through binding interactions with α2β1 integrin.[44,45] It has been reported that α3β1 is expressed at high levels in up to 77% of both low stage TaT1 papillary disease and high risk (T2-T4) disease samples tested, but in contrast to normal urothelium, is diffuse throughout the tumor and tumor surface.[45] Therefore, α3β1 on the surface of tumors would likely be accessible to VAX-IP minicells in the context of exophytic urothelial malignancy. Paradoxically, it has been shown that BCG acts to invade cells, a process shown to be required for immunotherapeutic benefit, through its interaction with α5β1 *in vivo*, despite the finding that this integrin subtype is not found in many NMIBC patient tumor samples.[46–48] However, there is some evidence to suggest that the localized inflammation of BCG causes upregulation of α5β1 in response to exposure of bladder cancer cell lines to the proinflammatory cytokine, IL-6, *in vitro*, a possible reason that no expression is seen in NMIBC tumor samples taken prior to BCG treatment where inflammation is not yet a factor.[49] A comprehensive analysis of α5β1 integrin expression profiles in NMIBC patients unresponsive to BCG has not been formally reported. It is conceivable that patients unresponsive to BCG lose the expression of α5β1 integrin or the ability to upregulate expression of α5β1 integrin due to dysfunctional IL-6 recognition, production, or signaling, yet retain the expression of mislocalized α3β1 integrin. If this were the case, VAX-IP minicells would have a distinct advantage as either salvage or first line treatment by virtue of its ability to target either integrin subtype.

Based on the preclinical *in vitro* and *in vivo* pharmacology results, mechanism of action, and general safety-tolerability observations recorded in the *in vivo* evaluation of this promising agent, VAX-IP minicells are well positioned for further nonclinical and clinical development and investigation in one or more NMIBC patient subpopulations and may have therapeutic benefit against a disease for which no new therapy has been approved for use in 25 years.

MATERIALS AND METHODS

Generation of minicell-producing strains

All strains used in this study are listed in Table 1. The wild-type K12 *Escherichia coli* minicell-producing strain, VAX8I3, contains a thermo-inducible genetic suicide mechanism described elsewhere.[17] The background *E. coli* minicell-producing strain was genetically engineered to be dependent upon diaminopimelic acid (DAP) for growth and to produce a detoxified form of LPS endotoxin by making sequential targeted chromosomal deletions of the *dapA* and *lpxM* genes using the phage λ Red recombinase system.[18] Briefly, each gene was independently targeted and deleted from the chromosome of MG1655 by the integration of a chloramphenicol resistance selection marker flanked by flipase (Flp) recognition target sequences for later removal after further introduction of the Flp recombinase expressing plasmid pCP20 as described 18. Once the deletion of the *dapA* gene had been confirmed by selection on chloramphenicol, phenotypic screening, and PCR analysis, the *dapA*- allele was transduced into a proline auxotroph (*proA*$^-$*B*$^-$) *E. coli* recipient strain by P1*vir* transduction. The *cat* gene was then removed by the Flp-mediated recombination of the flipase (Flp) recognition target sites flanking *cat* resulting in an antibiotic resistance-free *dapA*$^-$ recipient strain. The identical methodology was used to generate an *lpxM*- donor strain which was then used to transduce the *lpxM*- allele into the *dapA*-, *proA*$^-$*B*$^-$ recipient strain. Following removal of the *cat* marker using the Flp recombinase system, plasmid pVX-66, containing the minicell-producing IPTG inducible pTac::*ftsZ* gene construct fused to the *I-ceuI* genetic suicide mechanism and wild type proline biosynthesis genes was stably integrated into the *attB*λ site on the chromosome in the *proAB*$^-$, *dapA*$^-$, and *lpx*$^-$ strain and selected for on minimal media containing DAP as previously described.[17] The resulting strain, VAX12B4, was then confirmed to be temperature sensitive and dependent upon DAP for growth. The presence or absence of relevant genetic components was confirmed via PCR assays.

The gene sequences of the integrin-targeting bacterial adhesin protein, Invasin (*inv*), from *Yersinia pseudotuberculosis* and the putative cytotoxic protein payload, perfringolysin O (*pfo*) from *Clostridium perfringes* were synthesized as a transcriptional fusion via whole-gene synthesis and directionally cloned in parallel into a kanamycin-resistant version of the L-rhamnose-inducible bacterial expression plasmid, pRHA-67, to generate plasmids pVX-173, pVX-129, and pVX-156, respectively.[35,50,51] Following sequence confirmation, these plasmids were transformed into the minicell-producing strain VAX12B4, and clones selected for on MSB agar containing 50 µg/ml kanamycin, 10 µg/ml DAP, 111 µg/ml lysine, and 0.5% glucose at 30 °C to make minicell-producing strains VAX15D2 (*inv*-, *pfo*+), VAX13G8 (*inv*+, *pfo*-), and VAX14G8 (*inv*+, *pfo*+), respectively.

A streak plate of each minicell-producing strain was made on MSB agar containing 50 µg/ml kanamycin, 10 µg/ml DAP, 111 µg/ml lysine, and 0.5% glucose and grown at 30 °C, and isolated colonies used to inoculate starter cultures. Starter cultures were grown overnight in 50 ml of MSB liquid broth containing 50 µg/ml kanamycin, 10 µg/ml DAP, and 111 µg/ml lysine and grown at 30 °C with vigorous shaking at 230 rpm. On the following day, a minicell production culture was inoculated by 1:100 dilution of the starter culture into a larger volume of the same defined liquid growth media described above, then allowed to grow at 30 °C while shaking. Production cultures were monitored until reaching an optical density of 600 nm (OD_{600}) of 0.1 at which time they were induced for expression by the addition of L-rhamnose to a final concentration of 100 µmol/l. At an OD_{600} of 1.0, the minicell phenotype was induced by the addition of isopropyl β-D-1 thiogalactopyranoside (IPTG) to a final concentration of 1 mmol/l and the culture allowed to incubate overnight at 30 °C. On the following day, minicells were harvested by a combination of differential centrifugation steps and subsequent density gradient purification steps as previously described.[10–11]

Cells

Bladder cancer cell lines used in this study included the MB49 murine urothelial cell carcinoma, RT4 human urothelial cell carcinoma, HTB-9 human urothelial cell carcinoma, and the T24 human urothelial cell carcinoma cell lines. The MB49 and RT4 cell lines were maintained in Dulbecco's modified Eagle's medium (DMEM) with 10% heat inactivated fetal bovine serum, streptomycin and penicillin. The HTB-9 and T24 cell lines were maintained in RPMI-1640 supplemented with 10% fetal bovine serum, streptomycin and penicillin. All cell lines were maintained at 37 °C with 5% CO_2. Each cell line, with the exception of MB49, was purchased from American Tissue Type Collection (ATCC, Manassas, VA).

Hemolytic assay

Purified minicells were lysed by treatment with lysozyme and ethylenediaminetetraacetic acid (EDTA) in hypotonic conditions. Minicell lysates were serially diluted in PFO hemolysis buffer (phosphate-buffered saline (PBS) with 6 mmol/l L-cysteine and 100 µg/ml bovine serum albumin (BSA)) and added to 5×10^7 sheep red blood cells which were previously washed in hemolysis buffer in 96-well polypropylene microtiter plates. Plates were incubated at 37 °C with vigorous shaking for 1 hour, after which time any remaining red blood cells were pelleted by centrifugation and supernatants transferred to new 96-well microtiter plates to be analyzed for hemoglobin release as measured by absorbance at 540 nm (A_{540}). Hemolytic activity was compared to a standard curve generated using recombinant PFO (ATCC; BTX-100).

Western blot

Purified minicells were pelleted, resuspended in 25 µl of SDS-loading buffer, boiled for 10 minutes, 20 µl loaded onto a 12% SDS-PAGE Tris-glycine polyacrylamide gel (Life Technologies, Carlsbad, CA), and electrophoresis performed at 170 V for 1 hour. Once electrophoresis was complete, proteins

were transferred to nitrocellulose membrane using a Bio-Rad semi-dry transfer apparatus for 30 minutes at 5.5 mA/cm^2 nitrocellulose. Following transfer, nitrocellulose was incubated overnight in 10 ml of blocking buffer (PBS containing 1% BSA for PFO and 5% non-fat milk for Invasin). The following day, nitrocellulose was subject to three washes in PBS-T (PBS containing 0.2% Tween-20) for 5 minutes each. Mouse monoclonal antibody against Invasin (mAb3A2) or mouse monoclonal antibodies against PFO (mAb3H10) were used as primary detection reagents at 1:5,000 dilutions in blocking buffer. Following a 1-hour incubation with primary detection antibody, nitrocellulose was again washed three times in PBS-T prior to addition of the horseradish peroxidase-conjugated goat anti-mouse secondary antibody (Sigma Aldrich, St. Louis, MO). Following incubation with secondary detection antibody, nitrocellulose was again washed three times in PBS-T prior to addition of the Amersham ECL Prime Western Blotting Detection Reagent (GE Healthcare Life Sciences, Pittsburgh, PA). Images were captured using the BioSpectrum Imaging system (UVP, Upland, CA).

FACS analysis

For integrin surface expression analysis, cultured cells were detached by scraping from tissue culture flasks. Following detachment, 4×10^5 cells were harvested by centrifugation at 200×*g* for 5 minutes at 4 °C. Cell pellets were gently resuspended and then incubated with 2 µg of either anti-human β1 integrin antibody (MAB1956Z, Millipore, Billerca, MA), anti-human α5 antibody (MAB1987, Millipore), anti-human α3 antibody (mAb1952Z, Millipore, Billerica, MA) anti-mouse β1 integrin antibody (14-0291-81, eBioscience, San Diego, CA), or anti-mouse α5 antibody (553350, BD Biosciences) or no antibody for 1 hour at 4 °C. Cells were then gently washed three times each by centrifugation and resuspension, then incubated for 1 hour in the presence of either goat anti-mouse Alexa Fluor 488-conjugated secondary antibody or goat anti-hamster Alexa Fluor 488-conjugated secondary antibody (Life Technologies), as appropriate. Cells were washed three times each by centrifugation and analyzed for relative fluorescence activity compared to negative controls using a Stratedigm Flow Cytometer (Stratedigm, San Jose, CA).

For analysis of Invasin content on the surface of minicells, 2×10^9 minicells were incubated with 250 ng of mAb3A2 for 1 hour at room temperature while gently shaking. Minicells were then washed three times each by centrifugation and then incubated for 1 hour in the presence of a goat anti-mouse Alexa Fluor 488-conjugated secondary antibody (Life Technologies). Excess secondary detection antibody was removed by washing minicells three times each prior to analysis by flow cytometry.

Invasin-mediated minicell internalization assay

RT4, T24, and MB49 cells were seeded at a density of 10,000 cells/well in 12-well polystyrene tissue culture plates. On the following day, either VAX-I minicells (containing no PFO protein; *inv+, pfo-*) or native "vector" minicells generated from strain VAX12B4 (containing no Invasin or PFO; *inv-, pfo-*) were coincubated at a minicell to plated mammalian cell ratio (MOI) of 200:1 Following an incubation time of 2 hours, cells were then washed three times each in equal volumes of cell culture medium and assayed for minicell uptake by immunocytochemistry using a rabbit polyclonal antibody against *E. coli* minicells as the primary detection reagent. For fluorescence microscopy, cells were either fixed in 4% (w/v) paraformaldehyde for 20 minutes or fixed and permeabilized using 0.1% Triton X-100 immediately following incubation with fixative. For flow cytometry, cells were trypsinized before fixation or fixation and permeabilization. Whether adherent or enzymatically detached, following the fixation or fixation and permeabilization step(s), cells were washed three times each with PBS, then incubated with 250 ng/ml of the rabbit polyclonal antibody against *E. coli* minicells in PBS with 1% BSA. Following a 1-hour incubation at 4 °C, cells were washed three times each in PBS and then further incubated with Alexa Fluor 488-conjugated goat anti-rabbit secondary antibody (Life Technologies) in PBS with 1% BSA. Following 1 hour incubation at 4 °C, cells were washed three times, nuclei counterstained with 4′,6-diamidino-2-phenylindole (DAPI) (Life Technologies) at 5 µg/ml for 10 minutes followed by three washes, and then visualized by fluorescence microscopy (not performed for flow cytometry). All assays were performed multiple times on different days.

Assessing pyknotic nuclei of VAX-IP minicell-treated MB49 cells

MB49 cells were plated at a density of 5,000 cells per well in a 96-well polystyrene tissue culture plate and VAX-I and VAX-IP minicells were added at minicell to mammalian cell ratios of 6,000:1 and incubated at 37 °C. After a 24-hour incubation period, DAPI stain was added to the media at a final concentration of 5 µg/ml for 5 minutes. Following three successive washes in cell culture medium, DAPI-stained nuclei were imaged using a combination of fluorescence and bright-field microscopy.

Mitochondrial membrane potential assay

To determine any VAX-IP minicell-mediated loss in mitochondrial potential, MB49 cells were seeded in a 12-well polystyrene tissue culture plate at a density of 10^6 cells/well. Once cells were adherent, VAX-IP minicells were added at a minicell to mammalian cell ratio (MOI) of 6,000:1, centrifuged for 10 minutes at 670x*G*, and allowed to coincubate for 1 hour. Identical conditions using VAX-I as a control were evaluated in parallel. Following incubation, MitoTracker RedCMXRos (Molecular Probes, Eugene, OR) at a final concentration of 250 nmol/l/well and incubated for 1 hour at 37 °C in 5% CO_2. Cells were then scraped from the wells and centrifuged for 5 minutes at 1,500x*G*. The supernatant was aspirated and the pellet was resuspended in 1 ml of PBS and analyzed by fluorescence activated cell sorting (FACS) for a loss of fluorescent signal (E_x/E_m of 561/586 nm) as a measure of loss in mitochondrial membrane potential.

Caspase-3/7 activity assay

To test for VAX-IP minicell-mediated Caspase-3 and Caspase-7 activity, MB49 cells were seeded in a 96-well white-walled clear bottom polystyrene plate at a concentration of 5,000 cells/well and incubated for 3 hours. Once cells attached to the plate, VAX-IP minicells were added to the plate at an MOI of 5,000:1, and the plate was centrifuged for 10 minutes at 670×*g* before incubating overnight at 37 °C in 5% CO_2. The following day, a Caspase-Glo 3/7 assay was performed per the manufacturer's recommended protocol (Promega Corporation, Madison, WI). Caspase 3/7 activity was analyzed 30 minutes following addition of colorimetric substrate and compared to the caspase activity of untreated control cells.

PI staining

To analyze VAX-IP minicell-mediated membrane permeability and cell lysis, MB49 cells were seeded at a density of 10^6 cells/well in a 12-well polystyrene tissue culture plate and incubated for 4 hours in 37 °C with 5% CO_2 to allow for cell adhesion. Following adhesion, cells were treated with VAX-IP minicells, or VAX-I minicells as a negative control, both at a ratio of minicells to plated MB49 cell of 6,000:1. Plates were centrifuged at 670x*G* for 5 minutes and incubated for 2 hours prior to analysis. Cells were then scraped from the bottom of the wells, centrifuged at 2,000x*G* for 5 minutes, washed twice with PBS and resuspended in PBS containing propidium iodide at a concentration of 2 µg/ml. Additional negative control conditions included saline-treated controls as well as positive control conditions where cells were heated for 20 minutes at 55 °C. Cells were stained with PI for 15 minutes on ice and then analyzed using FACS (E_x/E_m of 561/586 nm).

In vitro cell viability assays

Cells were seeded into 96-well polystyrene plates at a density of 5,000 cells/well. On the following day, VAX-IP minicells or the appropriate VAX-I controls (*inv+, pfo-*) or VAX-P (*inv-, pfo+*), were added over a range of minicell to mammalian cell ratios (MOI) ranging from 10,000:1 to 3:1. Plates were briefly centrifuged for 5 minutes at 670x*G* and then allowed to incubate in the presence of minicells for 2–24 hours as described in the Results section and accompanying figures. Following incubation, cells were observed microscopically and then washed three times in cell culture medium. Unless indicated otherwise, cell viability was assessed at the 24 hours time point by the addition of 10 µl of PrestoBlue cell viability reagent (Life Technologies) directly to the cell culture medium, followed by a 3–5-hour incubation period to allow signals to develop. In control experiments designed to demonstrate the need for intact VAX-IP minicells to achieve tumor cell killing *in vitro*, a concentration of recombinant PFO (rPFO; BTX-100, ATCC) corresponding to that included in each amount of VAX-IP minicells used, or lysates of VAX-IP minicells corresponding to the concentration of intact VAX-IP minicells used for cell killing experiments, were exogenously added to cells. The IC_{50} value for each cell line was calculated by taking the concentration of test material to mammalian cells required to achieve half maximal signal as measured at E_x 560 nm/E_m 600 nm, per the manufacturer's specification. Each assay was run multiple times, in triplicate. Where indicated, integrin function-blocking antibodies (described in FACS Analysis section) were added at 10 µg/ml.

Lactate dehydrogenase release assay

RT4, T24, HTB-9, or MB49 cells were seeded into 96-well polystyrene plates at a density of 10,000 cells/well. On the following day, VAX-IP minicells or the appropriate VAX-I control were added over a range of minicell to mammalian cells ranging from 6,000:1 to 25:1. Plates were briefly centrifuged for 5 minutes at 670x*G* and then allowed to incubate in the presence of minicells in a time course up to 2 hours. At each time point, the cell culture supernatant was collected and separately assayed for lactate dehydrogenase (LDH) enzyme activity using the TOX7 LDH based In Vitro Toxicology Assay Kit as described by the manufacturer (Sigma Aldrich, St. Louis, MO).

Animals

Female C57BL/6 mice, 6–8 weeks of age, were used in all experiments and housed with normal bedding and chow with water *ad libitum* for the duration of the study under an animal protocol approved by the IACUC committee at Tulane University.

MB49 bladder cancer model and treatments

The establishment of syngeneic orthotopic tumors in the MB49 murine bladder cancer model was performed as described.[16,52] Briefly, mice were lightly anesthetized with isoflurane, the hair shaved from their lower backs, and electroconductive gel applied to the shaved area prior to being placed in dorsal recumbency on a grounding plate. Bladders were transurethrally catheterized using a sterile 24 gauge i.v. catheter with the stylet removed and drained of urine before insertion of a premeasured amount of platinum wire into the catheter. Cauterization was carried out via a short puls`e (~0.2 seconds) of low intensity (2.5W), monopolar, high frequency current, delivered by touching the exposed external portion of the wire with the cutting tool of a Bovie electrocautery unit (Bovie Medical Corporation, Clearwater, FL). After repositioning the catheter and guide wire against the bladder wall, a second cauterization was performed. The platinum guide wire was removed and mice were implanted with 100,000 MB49 cells in 100 µl of DMEM with 10% heat-inactivated fetal bovine serum. The catheter was allowed to remain in place for 90 minutes to prevent voiding and to ensure optimal tumor take. Tumor take rates were approximately 85% using this procedure. In preparation for receiving treatment, mice were lightly anesthetized with isoflurane and transuretherally catheterized using a lubricated 24 gauge i.v. catheter prior to intravesical administration of test agent. Intravesical treatments were instilled in 100-µl of sterile saline after which catheters were left in place to prevent voiding, allowing an overall treatment dwell time of 120 minutes.

In tumor growth experiments designed to find an effective dose range prior to entering into longer term survival studies, the more difficult-to-treat "late treatment" variation of the MB49 model was used. In these experiments, MB49 tumors were allowed to grow for 5 days, allowing orthotopic tumors to become well established and detectable by digital palpation and the presence of gross hematuria. Mice were randomized into treatment groups with seven to nine animals to group and treatment initiated on day 6 post-tumor installation and every 3 days thereafter (on days 9, 12, 15, and 18) for a total of five doses per subject. On day 19, all surviving subjects were euthanized, bladders extracted from each, and bladder weights measured and recorded as a surrogate indication of tumor burden, as is commonly practiced and reported with this model. Treatment groups included vehicle only (saline control), and VAX-IP minicells ranging from 5.0×10^6, 5.0×10^7, 1×10^8, 5×10^8, and 1×10^9 per dose.

In a first set of survival experiments using the late treatment variation of the MB49 model, tumors were again allowed to develop for 6 days before treatment initiation, as described above. Prior to the onset of treatments, mice were randomized into groups of six to eight animals each and intravesical treatments initiated on day 6 post-tumor installation with repeat intravesical dosing occurring every 3 days thereafter on days 9, 12, 15, and 18 (total of five doses). Using the dose range information gathered in previous experiments using this model variation, treatments included vehicle only (saline control), 1×10^8 VAX-IP minicells, or 5×10^8 VAX-IP minicells. Animals were weighed and observed daily for signs of systemic or local toxicity during a 60-day observation period. Following the 60-day observation period, the experiment was halted, surviving animals euthanized, and bladders removed to confirm the presence or absence of tumor via histological examination of sectioned bladders as compared to the bladders of animals that had succumbed to tumor burden during the study.

In a second set of survival experiments designed to compare VAX-IP minicells to what has been reported for BCG in the "early treatment" variation of the MB49 model, treatments were initiated 24 hours post-tumor instillation on day 1 and administered once weekly thereafter for 3 weeks on days 8, 15, and 22 (four doses total). Using the information gathered in the dose range finding study in combination with that used in the survival study employing the late treatment model variation, a dose of 1×10^8 VAX-IP minicells was compared to saline treated control. Following the 60-day observation period, the experiment was halted, surviving animals euthanized and bladders removed to confirm the presence or absence of tumor via histological examination of sectioned bladders as compared to the bladders of animals that had succumbed to tumor burden during the study.

Statistics

Cytokine data, caspase activation data, and integrin-blockade data were analyzed by one-way analysis of variance followed by Student *t*-test. Bladder weight data were analyzed for statistical significance compared to saline treated animals using the Mann-Whitney *U*-test. Kaplan-Meier survival curves were generated through the mathematical software GraphPad Prism, defining the event of interest as mouse death and the censored subjects as the mice that were still alive after 60 days. The horizontal axis represents survival time (days), and the vertical axis represents the percent survival at a certain time. Within each group, the two extreme values (subjects with the longest and shortest survival days) were excluded from the analysis. Survival data were analyzed for statistical significance using the log-rank test. Significance in all analyses performed was defined as a P value < 0.05

CONFLICT OF INTEREST

M.J.G. is employed by and holds an equity interest in Vaxiion Therapeutics in addition to being an inventor on relevant patent applications WO 2009/158364, WO 2012/112696, and WO/055682. W.T.G. declares no conflict of interest. R.A.S. is a shareholder in Vaxiion Therapeutics and the recipient of federal grant funding under 1 R44 NS087641-01 and 1RO3NS093291-01. S.T. is an employee of Vaxiion Therapeutics and a listed inventor on patent application WO 2009/158364. B.V. is a consultant to Vaxiion Therapeutics and declares no conflict of interest. X.C. declares no conflict of interest. B.H. declares no conflict of interest. K.R. is an employee of Vaxiion Therapeutics. V.H. is an employee of Vaxiion Therapeutics.

ACKNOWLEDGMENTS

The authors would like to thank Ralph Isberg at Tufts University for supplying the mAb3A2 antibody. The authors would also like to acknowledge that the mAb3H10 antibody reagent was provided by the Riken BRC through the National Bio-Resource Project of the MEXT, Japan. The authors also thank Kathleen McGuire at San Diego State University for her thoughtful review of the manuscript. This work was funded in part by the National Cancer Institute SBIR Phase 1 grant 1R43CA180403-1A1.

REFERENCES

1. Jemal, A, Bray, F, Center, MM, Ferlay, J, Ward, E and Forman, D (2011). Global cancer statistics. *CA Cancer J Clin* **61**: 69–90.
2. Ro, JY, Staerkel, GA and Ayala, AG (1992). Cytologic and histologic features of superficial bladder cancer. *Urol Clin North Am* **19**: 435–453.
3. Babjuk, M, Sylvester, R, Kaasinen, E, Bohle, A, Palou, J and Roupret, M (2012). Guidelines on non-muscle invasive bladder carcinoma (TaT1 and CIS) European Association of Urology.
4. Hall, MC, Chang, SS, Dalbagni, G, Pruthi, RS, Seigne, JD, Skinner, EC *et al*. (2007). Guideline for the management of nonmuscle invasive bladder cancer (stages Ta, T1, and Tis): 2007 update. *J Urol* **178**: 2314–2330.
5. Malmström, PU, Wijkström, H, Lundholm, C, Wester, K, Busch, C and Norlén, BJ (1999). 5-year followup of a randomized prospective study comparing mitomycin C and bacillus Calmette-Guerin in patients with superficial bladder carcinoma. Swedish-Norwegian Bladder Cancer Study Group. *J Urol* **161**: 1124–1127.
6. Berry, DL, Blumenstein, BA, Magyary, DL, Lamm, DL and Crawford, ED (1996). Local toxicity patterns associated with intravesical bacillus Calmette-Guérin: a Southwest Oncology Group Study. *Int J Urol* **3**: 98–100; discussion 101.
7. Deresiewicz, RL, Stone, RM and Aster, JC (1990). Fatal disseminated mycobacterial infection following intravesical bacillus Calmette-Guerin. *J Urol* **144**: 1331–3; discussion 1333.
8. Lamm, DL, van der Meijden, PM, Morales, A, Brosman, SA, Catalona, WJ, Herr, HW *et al.* (1992). Incidence and treatment of complications of bacillus Calmette-Guerin intravesical therapy in superficial bladder cancer. *J Urol* **147**: 596–600.
9. Steg, A, Leleu, C, Debré, B, Boccon-Gibod, L and Sicard, D (1989). Systemic bacillus Calmette-Guérin infection, 'BCGitis', in patients treated by intravesical bacillus Calmette-Guérin therapy for bladder cancer. *Eur Urol* **16**: 161–164.
10. Giacalone, MJ, Sabbadini, RA, Chambers, AL, Pillai, S, Berkley, NL, Surber, MW *et al.* (2006). Immune responses elicited by bacterial minicells capable of simultaneous DNA and protein antigen delivery. *Vaccine* **24**: 6009–6017.

11. Giacalone, MJ, Zapata, JC, Berkley, NL, Sabbadini, RA, Chu, YL, Salvato, MS *et al.* (2007). Immunization with non-replicating E. coli minicells delivering both protein antigen and DNA protects mice from lethal challenge with lymphocytic choriomeningitis virus. *Vaccine* **25**: 2279–2287.
12. MacDiarmid, JA, Mugridge, NB, Weiss, JC, Phillips, L, Burn, AL, Paulin, RP *et al.* (2007). Bacterially derived 400 nm particles for encapsulation and cancer cell targeting of chemotherapeutics. *Cancer Cell* **11**: 431–445.
13. Frazer, AC and Curtiss, R 3rd (1975). Production, properties and utility of bacterial minicells. *Curr Top Microbiol Immunol* **69**: 1–84.
14. Tweten, RK (1988). Nucleotide sequence of the gene for perfringolysin O (theta-toxin) from Clostridium perfringens: significant homology with the genes for streptolysin O and pneumolysin. *Infect Immun* **56**: 3235–3240.
15. Tweten, RK (1988). Cloning and expression in Escherichia coli of the perfringolysin O (theta-toxin) gene from Clostridium perfringens and characterization of the gene product. *Infect Immun* **56**: 3228–3234.
16. Günther, JH, Jurczok, A, Wulf, T, Brandau, S, Deinert, I, Jocham, D *et al.* (1999). Optimizing syngeneic orthotopic murine bladder cancer (MB49). *Cancer Res* **59**: 2834–2837.
17. Tsuji, S, Naili, I, Authment, NR, Segall, AM, Hernandez, V, Hancock, BM *et al.* (2010). An efficient thermoinducible bacterial suicide system: Eliminiation of viable parental bacteria from minicells. *BioProcess International* **8**: 28–40.
18. Datsenko, KA and Wanner, BL (2000). One-step inactivation of chromosomal genes in Escherichia coli K-12 using PCR products. *Proc Natl Acad Sci USA* **97**: 6640–6645.
19. Bukhari, AI and Taylor, AL (1971). Genetic analysis of diaminopimelic acid- and lysine-requiring mutants of Escherichia coli. *J Bacteriol* **105**: 844–854.
20. Yang, RB, Mark, MR, Gray, A, Huang, A, Xie, MH, Zhang, M *et al.* (1998). Toll-like receptor-2 mediates lipopolysaccharide-induced cellular signalling. *Nature* **395**: 284–288.
21. Chow, JC, Young, DW, Golenbock, DT, Christ, WJ and Gusovsky, F (1999). Toll-like receptor-4 mediates lipopolysaccharide-induced signal transduction. *J Biol Chem* **274**: 10689–10692.
22. Somerville, JE Jr, Cassiano, L, Bainbridge, B, Cunningham, MD and Darveau, RP (1996). A novel Escherichia coli lipid A mutant that produces an antiinflammatory lipopolysaccharide. *J Clin Invest* **97**: 359–365.
23. Leong, JM, Fournier, RS and Isberg, RR (1991). Mapping and topographic localization of epitopes of the Yersinia pseudotuberculosis invasin protein. *Infect Immun* **59**: 3424–3433.
24. Min, G, Stolz, M, Zhou, G, Liang, F, Sebbel, P, Stoffler, D *et al.* (2002). Localization of uroplakin Ia, the urothelial receptor for bacterial adhesin FimH, on the six inner domains of the 16 nm urothelial plaque particle. *J Mol Biol* **317**: 697–706.
25. Zhou, G, Mo, WJ, Sebbel, P, Min, G, Neubert, TA, Glockshuber, R *et al.* (2001). Uroplakin Ia is the urothelial receptor for uropathogenic Escherichia coli: evidence from *in vitro* FimH binding. *J Cell Sci* **114**(Pt 22): 4095–4103.
26. Nelson, LD, Johnson, AE and London, E (2008). How interaction of perfringolysin O with membranes is controlled by sterol structure, lipid structure, and physiological low pH: insights into the origin of perfringolysin O-lipid raft interaction. *J Biol Chem* **283**: 4632–4642.
27. Dang, TX, Hotze, EM, Rouiller, I, Tweten, RK and Wilson-Kubalek, EM (2005). Prepore to pore transition of a cholesterol-dependent cytolysin visualized by electron microscopy. *J Struct Biol* **150**: 100–108.
28. Decker, T and Lohmann-Matthes, ML (1988). A quick and simple method for the quantitation of lactate dehydrogenase release in measurements of cellular cytotoxicity and tumor necrosis factor (TNF) activity. *J Immunol Methods* **115**: 61–69.
29. Yeh, CJ, Hsi, BL and Faulk, WP (1981). Propidium iodide as a nuclear marker in immunofluorescence. II. Use with cellular identification and viability studies. *J Immunol Methods* **43**: 269–275.
30. Kroemer, G, Galluzzi, L and Brenner, C (2007). Mitochondrial membrane permeabilization in cell death. *Physiol Rev* **87**: 99–163.
31. Jacotot, E, Costantini, P, Laboureau, E, Zamzami, N, Susin, SA and Kroemer, G (1999). Mitochondrial membrane permeabilization during the apoptotic process. *Ann N Y Acad Sci* **887**: 18–30.
32. Isberg, RR and Leong, JM (1990). Multiple beta 1 chain integrins are receptors for invasin, a protein that promotes bacterial penetration into mammalian cells. *Cell* **60**: 861–871.
33. Isberg, RR and Tran Van Nhieu, G (1994). Binding and internalization of microorganisms by integrin receptors. *Trends Microbiol* **2**: 10–14.
34. Leong, JM, Fournier, RS and Isberg, RR (1990). Identification of the integrin binding domain of the Yersinia pseudotuberculosis invasin protein. *EMBO J* **9**: 1979–1989.
35. Isberg, RR, Voorhis, DL and Falkow, S (1987). Identification of invasin: a protein that allows enteric bacteria to penetrate cultured mammalian cells. *Cell* **50**: 769–778.
36. Van Nhieu, GT and Isberg, RR (1991). The Yersinia pseudotuberculosis invasin protein and human fibronectin bind to mutually exclusive sites on the alpha 5 beta 1 integrin receptor. *J Biol Chem* **266**: 24367–24375.
37. Zhang, X, Atala, A and Godbey, WT (2008). Expression-targeted gene therapy for the treatment of transitional cell carcinoma. *Cancer Gene Ther* **15**: 543–552.
38. Zhang, X, Turner, C and Godbey, WT (2009). Comparison of caspase genes for the induction of apoptosis following gene delivery. *Mol Biotechnol* **41**: 236–246.
39. Zhang, X and Godbey, WT (2011). Preclinical evaluation of a gene therapy treatment for transitional cell carcinoma. *Cancer Gene Ther* **18**: 34–41.
40. Lamm, DL, Reichert, DF, Harris, SC and Lucio, RM (1982). Immunotherapy of murine transitional cell carcinoma. *J Urol* **128**: 1104–1108.
41. Shintani, Y, Sawada, Y, Inagaki, T, Kohjimoto, Y, Uekado, Y and Shinka, T (2007). Intravesical instillation therapy with bacillus Calmette-Guérin for superficial bladder cancer: study of the mechanism of bacillus Calmette-Guérin immunotherapy. *Int J Urol* **14**: 140–146.
42. Chwieralski, CE, Welte, T and Bühling, F (2006). Cathepsin-regulated apoptosis. *Apoptosis* **11**: 143–149.
43. Kim, C, Patel, P, Gouvin, LM, Brown, ML, Khalil, A, Henchey, EM *et al.* (2014). Comparative analysis of the mitochondrial physiology of pancreatic β cells. *Bioenergetics* **3**: 110.
44. Behnsawy, HM, Miyake, H, Abdalla, MA, Sayed, MA, Ahmed, Ael-F and Fujisawa, M (2011). Expression of integrin proteins in non-muscle-invasive bladder cancer: significance of intravesical recurrence after transurethral resection. *BJU Int* **107**: 240–246.
45. Liebert, M, Washington, R, Stein, J, Wedemeyer, G and Grossman, HB (1994). Expression of the VLA beta 1 integrin family in bladder cancer. *Am J Pathol* **144**: 1016–1022.
46. Zhao, W, Schorey, JS, Bong-Mastek, M, Ritchey, J, Brown, EJ and Ratliff, TL (2000). Role of a bacillus Calmette-Guérin fibronectin attachment protein in BCG-induced antitumor activity. *Int J Cancer* **86**: 83–88.
47. Zhao, W, Schorey, JS, Groger, R, Allen, PM, Brown, EJ and Ratliff, TL (1999). Characterization of the fibronectin binding motif for a unique mycobacterial fibronectin attachment protein, FAP. *J Biol Chem* **274**: 4521–4526.
48. Kuroda, K, Brown, EJ, Telle, WB, Russell, DG and Ratliff, TL (1993). Characterization of the internalization of bacillus Calmette-Guerin by human bladder tumor cells. *J Clin Invest* **91**: 69–76.
49. Zhang, GJ, Crist, SA, McKerrow, AK, Xu, Y, Ladehoff, DC and See, WA (2000). Autocrine IL-6 production by human transitional carcinoma cells upregulates expression of the alpha5beta1 firbonectin receptor. *J Urol* **163**: 1553–1559.
50. Giacalone, MJ, Gentile, AM, Lovitt, BT, Berkley, NL, Gunderson, CW and Surber, MW (2006). Toxic protein expression in Escherichia coli using a rhamnose-based tightly regulated and tunable promoter system. *Biotechniques* **40**: 355–364.
51. Shimizu, T, Okabe, A, Minami, J and Hayashi, H (1991). An upstream regulatory sequence stimulates expression of the perfringolysin O gene of Clostridium perfringens. *Infect Immun* **59**: 137–142.
52. Dobek, GL and Godbey, WT. (2011) An orthotopic model of murine bladder cancer. *J Vis Exp* **48**: 2535.